Volume 17 Number 16 1989 Nucleic Acids Research

Analysis of polyadenylation site usage of the c-*myc* oncogene

Ite A.Laird-Offringa, Peter Elfferich, Heleen J.Knaken, Joke de Ruiter and Alex J. van der Eb

Laboratory for Molecular Carcinogenesis, Sylvius Laboratories, University of Leiden, The Netherlands

Received June 13, 1989; Accepted July 10, 1989

ABSTRACT

The c-*myc* gene contains 2 well conserved polyadenylation (pA) sites. In all human and rat cell lines from various differentiation stages and tissue types the amount of mRNA terminating at the second pA site is 6-fold higher than the amount ending at the upstream site. This is not due to a difference in stability of the two mRNA types and therefore must be due to preferential usage of the downstream site. The usage of the pA sites is not altered during growth factor induction of quiescent cells. We have not been able to detect differences in behavior between mRNAs ending at either pA site. Both types of mRNA are induced upon treatment of cells with cycloheximide. Furthermore, we have shown that the poly(A) tail of c-*myc* mRNA is lost during degradation of the messenger, as was described previously for c-*myc* mRNA in an *in vitro* system. The time required for the loss of the poly(A) tail is similar to the the half-life of c-*myc* mRNA.

INTRODUCTION

Since the discovery of oncogenes there has been a great interest in the regulation of their expression. Much research has been focused on the 5′ region of these genes. Studies of the c-*myc* oncogene, for example, revealed the presence of two differentially used promoters (1), positive and negative regulatory elements (2,3) and a transcription elongation block near the end of the first exon (4,5). Recently, research has also been focused on the 3′ region of a number of oncogenes, primarily due to the discovery that (A+T)-rich regions just upstream of the polyadenylation (pA) signal seem to influence mRNA stability. These (A+T)-rich regions were first described by Caput *et al.* (6). Shaw and Kamen (7) showed that the (A+T)-rich region of the granulocyte-monocyte-colony-stimulating factor (GM-CSF) gene, upon introduction into the β-globin gene, specifically reduced the half-life of the normally stable β-globin mRNA. Furthermore, they showed that similar (A+T)-rich regions are present in other growth factor (GF) genes and in several oncogenes, among which c-*myc* and c-*fos*. Both c-*myc* and c-*fos* belong to a set of strictly regulated GF-inducible genes (8,9) and produce very unstable mRNAs (10,11,12). For each of these oncogenes, the 3′ (A+T)-rich regions of the genes have been shown to play a role in conferring the instability on the corresponding mRNAs (13,14,15). However, more upstream regions also seem to be involved (13,16) and the exact role of the (A+T)-rich regions remains to be elucidated. In this respect, the c-*myc* gene is very interesting. It contains not one, but two pA signals, each preceded by an (A+T)-rich region (17,18). The presence of two pA signals is not uncommon. In one study (19) a repetition of the AATAAA motif was observed in 30% of the genes studied. In those cases, however, the two pA signals were located within 30 basepairs (bp) of each other and only one 3′ terminus was formed. Several genes in which multiple pA signals do give rise to transcripts with different 3′

termini have also been described (20). In at least two of these genes, pA signals have been shown to be differentially utilized. The pA site usage of the chicken vimentin gene is modulated during embryonic development (21). The mouse dihydrofolate reductase (DHFR) gene contains four different pA signals that are differentially used in resting and growing cells (22). In the c-*myc* gene the pA signals are 150 bp apart, each one followed by its own poly-adenylic acid (poly(A)) addition site. Although both the pA signals and the preceding (A+T)-rich regions are well conserved between rat and human, in the cell lines analyzed to date the second pA site is used most frequently if not exclusively. Thus, most c-*myc* mRNAs contain two (A+T)-rich regions whereas a minor fraction contains only one. This raises the interesting possibility that the use of the different pA sites may have a regulatory function. Until now, no detailed analysis of c-*myc* pA site usage in cells from different lineages or under different growth conditions has been presented. The aim of our study was to measure pA2/pA1 ratios in several human and rat cell lines and to look for differences in behavior between the messengers terminating at either pA site. We have determined the half-life of these mRNAs and have analyzed pA site usage during GF induction. Additionally, we have studied whether c-*myc* mRNA stabilization by inhibitors of protein synthesis (as first described by Linial *et al.* (23)) occurs to the same extent for mRNAs with different 3′ termini and whether the poly(A) tail is shortened during mRNA decay, as was described for c-*fos* (24) and in an *in vitro* system for c-*myc* (25).

MATERIALS AND METHODS

Computer analyses

Sequences from the GenBank or from the EMBL DNA data banks were compared with the program GAP of the Wisconsin Software Package (41).

Cell lines

VH10 cells (human foreskin fibroblasts) and VH10-SV cells (VH10 cells transformed with the SV40 early region(26)) were grown in Ham's F-10 medium containing 10% fetal calf serum (FCS). HeLa, human embryonic retina (HER) and COLO 320 (a colon cancer cell line that contains rearranged and amplified c-myc genes (27)) cells were grown in minimal essential medium (MEM) containing 10% fetal calf serum (FCS). Rat-2 fibroblasts (28), NRK cells (normal rat kidney clone 49F (29)) and polyomavirus-transformed rat embryo fibroblasts (REF-PY; generously donated by F. Cuzin, Nice, France) were grown in minimal essential medium (MEM) containing 10% newborn calf serum (NCS). The 511 and 223 cell lines are Rat-2 derivatives containing 1 and 2 copies of the intact human c-*myc* gene respectively (*Hin*dIII-*Eco*RI fragment, a plasmid containing this fragment was kindly provided by S. Cory, Melbourne, Australia (30)). The 534.15 and 534.10 cell lines were obtained by transfecting Rat-2 cells with a plasmid containing a chloramphenicol acetyl transferase (CAT)-*myc* fusion gene (see below). RNA from human embryonal lung (HEL) cells and from M13 cells (a small-cell lung carcinoma cell line containing a c-*myc* amplification) were generously provided by M. Wurfbain. RNA from the human acute lymphocytic leukemia cell line MOLT4 was kindly donated by T. Berkvens. RNA from baby rat kidney (BRK) cells was a gift of M. Timmers.

RNA isolation

Cytoplasmic RNA was isolated using the NP-40 detergent method (31).

mRNA stability assays and cycloheximide induction

1−2 days before the experiment cells were seeded on 15-cm plates. For the stability assays

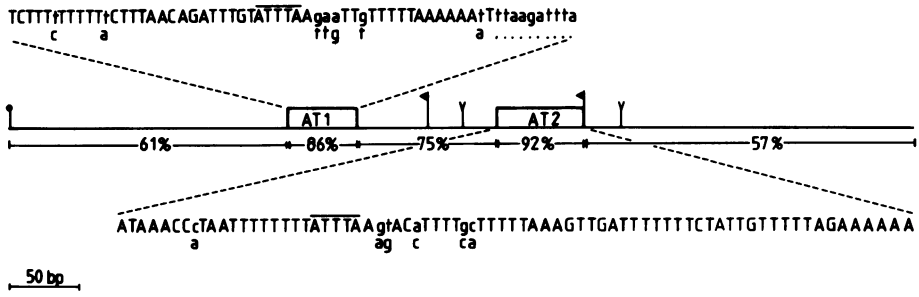

Figure 1. Schematic representation of the conserved 3′ region of the c-*myc* gene. The percentage homology between rat and human of the various regions is given. The 86% given for the AT1 region does not take into account that the human AT1 is slightly longer. The sequences of both human (A+T)-rich regions are shown. The sequence of the human gene is given in the top line. Non-conserved nucleotides are printed in small letters with the corresponding nucleotides in the rat underneath. Absence of corresponding nucleotides in the rat is denoted by a dot beneath the human sequence. AT1, AT2: first and second (A+T)-rich regions; lollipop: translation stop codon; black flag: pA signal (AATAAA); fork: poly(A) addition site.

actinomycin D was added at zero time to a final concentration of 5 μg/ml. Actinomycin D stocks (2 mg/ml) not older than 2 weeks were used. For cycloheximide (CH) induction, CH was added to subconfluent cell cultures to a final concentration of 10 μl/ml. After 1 hour actinomycin D was added to half of the plates (5 μg/ml). RNA was isolated at the desired timepoints.

Plasmid constructs

The CAT-*myc* construct was made by inserting a blunted 535-bp *Dde*I fragment containing both human c-*myc* p(A) signals into the *Hpa*I site of the E/P-CAT plasmid. E/P-CAT contains the *Hind*III-*Bam*HI fragment of pSV2CAT (containing the CAT gene, the SV40 large T splice site and the SV40 early p(A) signal (32) cloned into the *Hin*dIII/*Dde*I sites of pUC12 and the SV40 early enhancer/promoter *Pvu*II-*Hin*dIII fragment inserted into the *Bam*HI/*Hin*dIII sites 5′ of the CAT gene. The resulting CAT-*myc* construct contained both c-*myc* p(A) signals followed by the SV40 p(A) signal at a distance of 250 bp. For RNase protection analysis genomic 3′ fragments of the human and the rat c-*myc* gene were cloned into plasmids containing the SP6 promoter. For the human probe a 535-bp *Dde*I fragment spanning both p(A) sites was cloned into pEP40 (an SP6 promoter-containing plasmid provided by P.W. Laird) in antisense orientation compared to the SP6 promoter. For the rat probe, a 707-bp *Xho*I-*Pst*I fragment, from a plasmid kindly provided by G. Klein, Stockholm, was cloned into pEP30 (polylinker reversed compared to pEP40) in antisense orientation. Control plasmids were a 140-bp *Hin*fI fragment of the rat glyceraldehyde phosphate dehydrogenase (GAPDH) cDNA (34) and a 117-bp *Hae*III fragment of the human elongation factor 1a (HEF) cDNA (35) cloned in antisense orientation into pEP30. Before SP6 transcription the plasmids were linearized by cutting at a restriction site 3′ to the insert.

RNase protection analysis

Synthesis of [^{32}P]-UTP labeled RNA probes, hybridization and digestion was generally done according to the Promega Riboprobe protocol, with minor alterations. 0.5 μg linearized plasmid was used as a template, with 13 mM [^{32}P]-UTP plus 30 mM cold UTP for myc probes and 2 mM [^{32}P]-UTP plus 40 mM cold UTP for control probes. The probes were kept in a 200 μl ethanol suspension. 5−10 μl probe was added to each 20 μg cytoplasmic

RNA (or control tRNA) sample. After coprecipitation RNA was dissolved in hybridization mix (80% formamide, 0.4 M NaCl, 1 mM EDTA, 40 mM Pipes pH 6.7) and hybridized overnight at 37°C. Samples were digested for 60 min. at 30°C in 300 μl RNase buffer (10 mM Tris/HCl pH 7.5, 5 mM EDTA, 0.3 mM NaCl) containing 1.5 units of RNase T1 (Promega). Following purification and precipitation the samples were dissolved in 2 μl TE (10 mM Tris-HCl pH 8.0, 1 mM EDTA) plus 8 μl formamide. 2 μl layer mix (15% ficoll in water and tracking dye) were added, the samples were denatured at 85°C and run on a denaturing 5% polyacrylamide/urea gel.

The poly(A) tail degradation experiments were performed as described above. Following digestion and purification, ethanol-precipitated pellets were dissolved in 6 μl TE. The samples were then divided equally between 2 tubes. Formamide and tracking dye was added to the samples for the denaturing gel. 3 μl layer mix containing 0.5% SDS was added to the other samples. The latter were loaded directly onto a (cool) non-denaturing 5% polyacrylamide gel (lacking urea).

Densitometrical scanning and scintillation counting

To quantitate bands by densitometrical scanning, autoradiograms exposed within the linear range of the film were scanned on a Biorad densitometer. A mathematical program was used to integrate the area under each peak. To compare bands greatly differing in intensity, the bands were cut out from the gel and eluted overnight at 37°C in 200 μl 0.1 M NaOH. Prior to counting 2.5 ml Packard Scintillator 299 cocktail was added. The samples were counted 3 times for 10 min. For each band a piece of gel of the same size just above or below the band was cut out to quantitate the background counts. The value obtained was subtracted from the counts in the sample containing the band.

RESULTS

Conservation of pA signals and (A+T)-rich regions in human and rat c-myc genes

Both the human and rat c-*myc* genes have been sequenced well beyond the second pA signal (17,18,33). We have used these two sequences to look for conserved regions in the 3′ end of the c-*myc* gene, using a computer alignment program (41). The overall sequence conservation of the non-coding exon 1 is about 70%, while the coding sequences (exons 2 and 3) are about 88% conserved (33). The 3′ untranslated part of the gene is conserved for only about 65%. A more accurate study of this region (summarized in Figure 1) reveals that the 3′ region contains two highly conserved stretches: the (A+T)-rich regions. The first of these regions (AT1) lies 60 bp (human) or 40 bp (rat) upstream of pA1 and is 86% conserved. This A+T stretch in the human gene is slightly longer than the one in the rat gene. The second (A+T)-rich region (AT2) abuts the second pA signal and is 92% conserved. Though both AT1 and AT2 have a comparable A+T content (83−88%) their sequences clearly differ. Comparison of AT1 and AT2 within one species shows a homology of less than 60%.

pA1 and pA2 usage in cell lines from different lineages

A summary of published data concerning the use of the different c-*myc* pA signals is given in Table I. No mRNA terminating at pA1 was detectable in any rat or chicken cells examined. In all human cell lines studied, pA2 was used much more frequently than pA1. The only instance in which pA2 was not used predominantly or exclusively, was when the human c-*myc* gene was expressed in *Xenopus* oocytes. In that case both pA sites were used with equal efficiency. This raises the question whether pA usage is specifically regulated by cellular factors that determine the affinity of the poly(A) addition machinery for each

TABLE I
SUMMARY OF PUBLISHED DATA CONCERNING c-*myc* pA SITE USAGE

NAME	CELL TYPE	pA2	pA1	REF.[A]
HUMAN				
K562	erythroleukemia cell line	+++	+	25
HL60	promyelocytic leukemia cell line	+++	+	36
BL2	Burkitt lymphoma cell line	~20	1	37
Daudi	Burkitt lymphoma cell line	~20	1	37
ST486	Burkitt lymphoma cell line	~20	1	37
RAT				
–	normal liver	+	–	33
–	regenerating liver	++	–	33
–	normal spleen	+	–	33
7794A	Morris hepatoma	+++	–	33
CHICKEN				
CEF	embryo fibroblasts	++	–	38
LL7	bursal lymphoma	+++	–	38
OTHER				
–	Xenopus oocytes containing the human c-*myc* oncogene	+++	+++	37

A: numbers refer to references listed at the back of the manuscript.

pA site or by topological factors such as the distance between the pA sites. Therefore we analyzed an array of human and rat cell lines from different lineages. Uniformly labeled RNA probes (see Figure 2) were hybridized to 20 μg cytoplasmic RNA in an RNase protection assay. To prevent the formation of artefactual bands due to non-specific cleavage by RNase A in the (A+U)-rich regions (not shown), only RNase T1 was used in the digestion reaction. Under these conditions a double band is seen at the position where the human pA2 protected fragment is expected, presumably due to either heterogeneity of the second poly(A) addition site or to incomplete cleavage by RNase T1, which is G specific. Heterogeneity of the downstream human pA site has been described by Brewer and Ross (25). The use of higher concentrations of RNase T1 did not lead to a decrease of either band. Therefore both bands were considered to represent mRNAs terminating at pA2. Because the amount of c-*myc* mRNA differed considerably between the various cell lines, the RNase protection analysis was performed with varying amounts of cytoplasmic RNA, depending on the c-*myc* expression level (Figure 3A). The autoradiograms were scanned densitometrically to determine the ratio of pA2 to pA1 usage. To get more accurate values for the pA2/pA1 ratio, the bands were cut out from the gels and the radioactivity

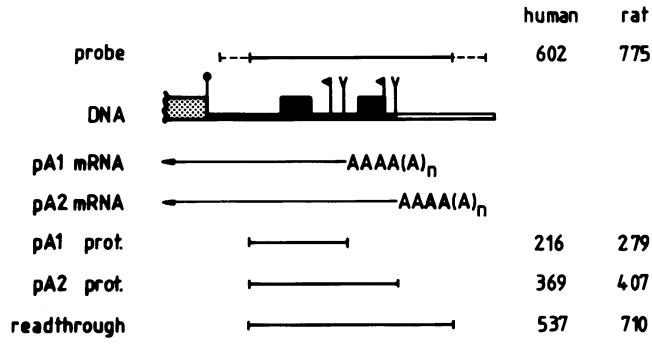

Figure 2. 3′ c-*myc* probes used for RNase protection. The lengths of the probes and protected RNA fragments for human and rat are given in nucleotides at the right side of the figure. Broken line: polylinker sequences present in the probe; dotted box: exon 3 translated sequences; black bar: sequences present in mRNA; black boxes: (A+T)-rich regions; lollipop, black flag and fork: as in Figure 1.

in each band was measured using a scintillation counter. Due to the fact that we used a probe uniformly labeled with UTP, the pA2 fragments contained approximately 1.6 times more label. After correction for this factor the resulting pA2/pA1 ratios are as given in Table II. Despite the large differences in c-*myc* expression between the various cell types, the proportion of messengers ending at pA2 and pA1 did not vary significantly. Apparently mRNAs ending at the second pA site are more abundant in all embryonic and mature cells tested, including several neoplastic cells. Contrary to the findings of Hayashi *et al.* (33), we could detect a weak band of about 280 nucleotides corresponding to rat c-*myc* mRNA ending at pA1 (Figure 3C). The band was present in all rat cell lines tested. We also detected a band of about 220 nucleotides. While the pA1 band was always detectable the 220 band was not reproducibly present. There is no pA signal upstream of pA1. Sometimes we also found an extra band (of 150 nucleotides) when analyzing human RNA. The extra bands became more intense when more RNase T1 was used (not shown). Therefore we presume they are degradation products of the upper bands. The ratio of pA2 to pA1 was estimated to be about 6 in all rat cells examined (Table II). Thus the relative use of the two pA sites appears to be approximately the same in human and rat cells. The RNA of two Rat-2 cell lines containing one or two intact copies of the human c-*myc* gene was also analyzed. In these cell lines exactly the same poly(A) addition sites as in the human cells were used and the ratio was comparable to that in human cells. The analysis of one of the cell lines, 511, is shown in Figure 3A, lane 8. To study the effect of an additional pA signal downstream of c-*myc*, we analyzed the RNA of Rat-2 cells transfected with a CAT gene linked to a c-*myc* fragment containing both pA signals followed by the SV40 late pA signal (Figure 3B, lane 2). In two independent monoclonal cell lines about 20% of the CAT-*myc* fusion mRNA does not end at a c-*myc* pA site. This fraction of the RNA gives rise to a protected fragment of 537 nucleotides (see Figure 2). While the intensity of the pA1 protected band seems alike in lanes 1 and 2 of Figure 3B, the amount of pA2 band in lane 2 is less than in lane 1. Apparently the pA2/pA1 ratio in the celline containing the hybrid construct is altered. The presence of the SV40 pA signal downstream of the c-*myc* pA signals appears to influence the amount of transcripts terminating at pA2.

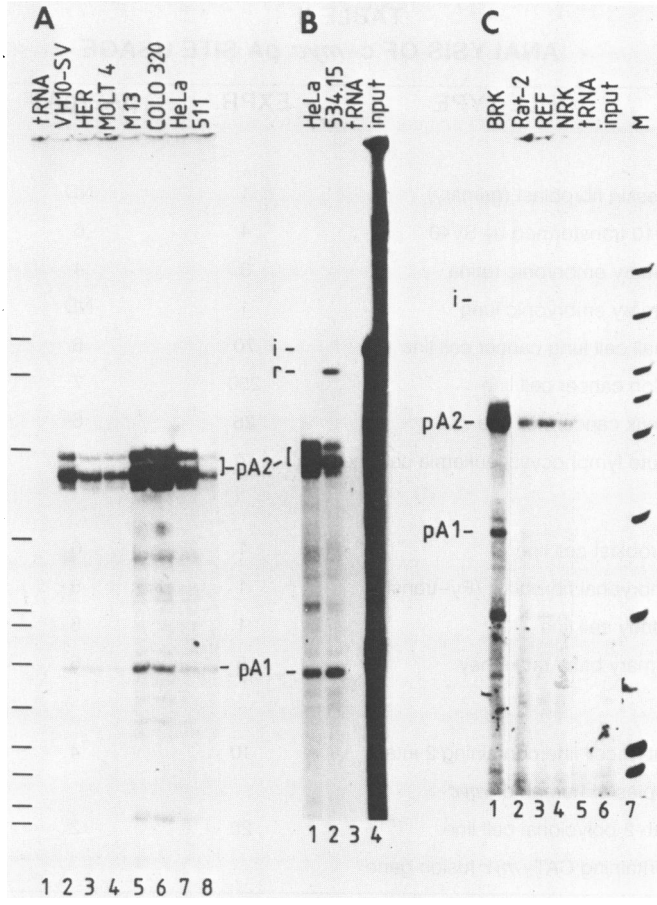

Figure 3. RNase protection analysis with RNA from human and rat cell lines with 3′ c-*myc* probes. tRNA was added to samples containing less than 20 μg RNA. **A.** Different amounts of cytoplasmic RNA were hybridized to the human 3′ probe: lane 1: tRNA, 20 μg; 2: VH10-SV, 50 μg; 3: HER, 50 μg; 4: Molt 4, 20 μg; 5: M13, 5 μg; 6: COLO 320, 2 μg; 7: HeLa, 10 μg; 8: 511, 10 μg. Marker: pBR322×*Hpa*II (622, 527, 404, 309, 242, 238, 201, 190, 180, 160, 140 nucleotides). Exposure: 14 hrs. **B.** The human 3′ probe was hybridized to 20 μg HeLa RNA (lane 1) and 20 μg 534.15 RNA (lane 2). Lanes 3: tRNA; 4: input probe. i: input; r: readthrough. Exposure: 4 days. **C.** 20 μg cytoplasmic RNA from rat cells was hybridized to the rat probe (lanes 1−4). The REF cells used were transformed by Polyomavirus. Lanes 5: tRNA; 6: input probe; M: marker, starting from third band from top: 517, 454, 396, 298, 220, 154, 145 nucleotides. Exposure: 16 hrs.

Half-life and stabilization of c-myc mRNA

A possible explanation for the different amounts of c-*myc* mRNA ending at pA1 and pA2 could be that the half-life of the smaller transcript is shorter, leading to lower steady-state levels of this mRNA. To test this possibility we blocked mRNA synthesis by the addition of actinomycin D and isolated cytoplasmic RNA at several timepoints. HeLa cells were used for this experiment because they have a relatively high c-*myc* expression, making mRNAs ending at pA1 more easily detectable. RNA samples were simultaneously hybridized to the 3′ *myc* probe and the human elongation factor (HEF) control probe .

TABLE II
ANALYSIS OF c-*myc* pA SITE USAGE

NAME	CELL TYPE	EXPR.[A]	pA2/pA1[B]	FIGURE[C]
HUMAN				
VH10	foreskin fibroblast (primary)	1	ND	NS
VH10-SV	VH10 transformed by SV40	4	6	3A
HER	primary embryonic retina	3	4	3A
HEL	primary embryonic lung	1	ND	NS
M13	small cell lung cancer cell line	70	6	3A
COLO 320	colon cancer cell line	250	7	3A
HeLa	cervix cancer cell line	25	6	3A
Molt4	acute lymphocytic leukemia cell line	7	6	3A
RAT				
Rat-2	fibroblast cell line	1	6	3C
REF-Py	embryonal fibroblast (Py-transf.)	1	6	3C
NRK	kidney cell line	1	6	3C
BRK	primary baby rat kidney	5	6	3C
OTHER				
511	Rat-2 cell line containing 2 intact copies of human c-*myc*	10	4	3A
543.15	Rat-2 polyclonal cell line containing CAT-*myc* fusion gene	25	2	3B

A: c-*myc* relative expression level, in rat cells as compared to Rat-2 cells, in all other cells as compared to VH10 cells. B: ratio of pA2 to pA1 usage. ND means the signal from the cell line was too weak to measure this ratio. For the ND cell lines the ratio seemed comparable to the other cell lines. C: refers to the figure containing the RNase protection data pertaining to each cell line. NS means not shown: the signal of c-*myc* in these cells was extremely weak and only visible after very long exposure times, causing a high background level.

The result is shown in Figure 4A. The half-lives of pA1 and pA2 mRNAs were calculated by plotting the logarithm of the amount of remaining signal against the time (Figure 4B). Small differences in the amount of RNA used for each lane were corrected by using the probe for HEF mRNA (which has a half-life of more than 6 hrs.) as a reference. The RNase protection was done with RNA samples from 3 independent experiments. The calculated mean values for the half-lives of pA1 and pA2 mRNA were : 13 ± 4 min. for pA2 mRNA and 20 ± 9 min. for pA1 mRNA. Thus we may conclude that both mRNAs are equally unstable, with a half-life of about 15 min. The half-life of total c-*myc* mRNA in Hela cells as determined by Northern blot analysis is 10−15 min. (not shown). In a

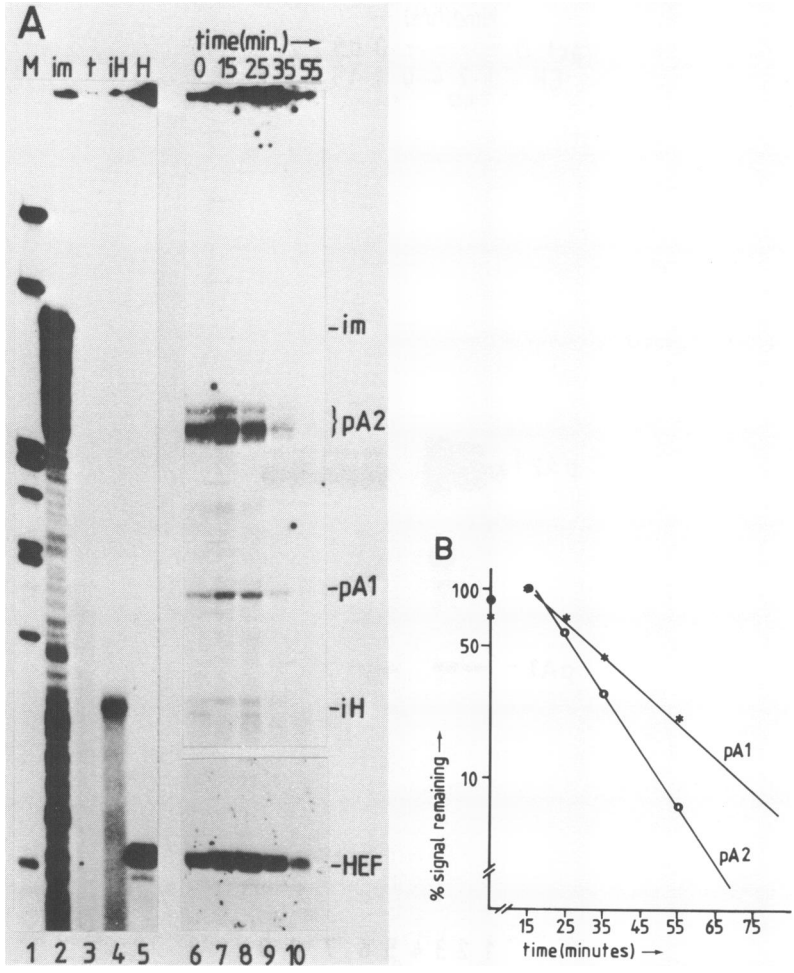

Figure 4. A. RNase protection analysis of actinomycin D-treated HeLa cells. 20 μg cytoplasmic HeLa RNA was hybridized simultaneously to the human 3′ c-*myc* probe and the HEF probe (lanes 6−10). M: marker pBR322×*Sau*IIIA (1374, 665, 358, 341, 317, 272, 258, 207, 105 nucletides); im: input *myc* probe; t: tRNA; iH: input HEF probe; H: HeLa RNA with HEF probe only. Exposure: 2 days. Inset: shorter exposure of HEF control bands, 14 hrs. **B.** The percentage remaining signal plotted logarithmically against the time. The bestfit lines were calculated using linear regression. In this graph the calculated half-lives are: pA2: 8 min. (correlation coeff. (r^2) 1.0) and pA1: 15 min. (r^2= 1.0). The values of 2 other plots from independent experiments were pA2: 15 min. (r^2= 0.97) and 15 min. (r^2= 1.0); pA1: 30 min. (r^2= 0.98) and 15 min. (r^2= 0.99). From these values the mean half-lives were calculated to be 13 ± 4 min. (pA2) and 20 ± 9 min. (pA1).

comparable experiment with NRK cells the half-life of pA2 and pA1 mRNA was also determined to be about 15 min. (not shown). Thus the comparatively low levels of pA1 mRNA are not caused by its relative instability.

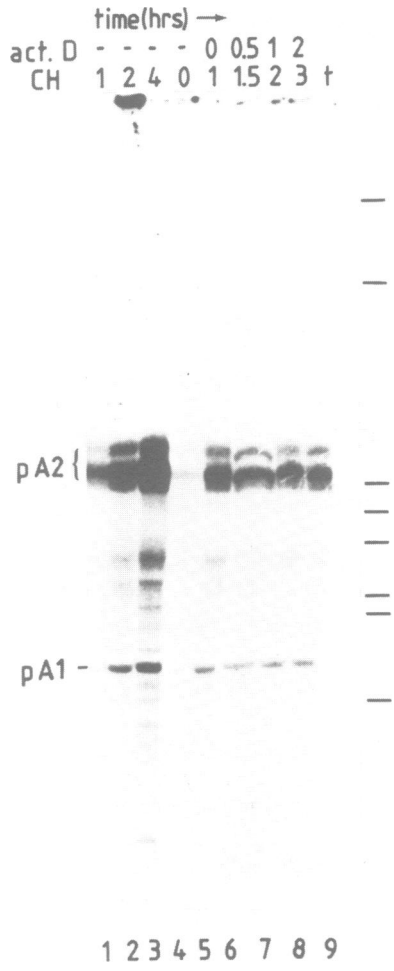

Figure 5. RNase protection analysis of CH- and actinomycin D-treated HeLa cells. 20 μg cytoplasmic RNA was hybridized to the human 3′ c-*myc* probe. Lanes 1–3: cells treated with CH only. Lane 4: untreated cells. Lanes 5–9: after 60 min. CH treatment actinomycin D was added. t: tRNA control. Marker: pBR322×*Sau*IIIA (see legend Figure 4). Exposure: 5 hrs.

The fact that c-*myc* messengers ending at pA1 and pA2 have comparable half-lives under the conditions studied, does not exclude that there may be instances in which the stability of mRNAs ending at either site could be altered. Not much is known about the regulation of mRNA stability. It has been described that mRNAs from certain genes, among which c-*myc* (23), are stabilized by drugs that inhibit protein synthesis. Whether this is the case for all c-*myc* mRNAs was not clear. Therefore, we analyzed c-*myc* mRNA from HeLa cells treated with cycloheximide (CH), in the presence or absence of actinomycin D. Upon addition of CH, levels of both pA1 and pA2 mRNA increase (Figure 5, lanes 1–3). When actinomycin D is added after a preincubation of 60 min. with CH, the levels of these RNAs

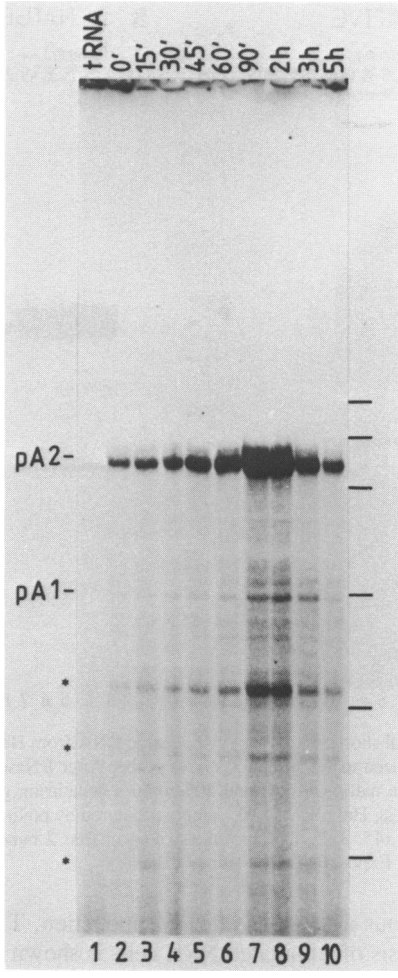

Figure 6. RNase protection analysis of GF-induced NRK cells. 20 μg cytoplasmic NRK RNA was hybridized to the rat 3' c-*myc* probe. The time after GF inducion is given at the top of the figure. Background bands (which are higher than normal due to a slight overdose of RNase T1) are marked by stars. Marker: 517, 454, 396, 298, 220, 154 nucleotides. Exposure: 14 hrs.

hardly decrease during 2 hours (compare Figure 5, lanes 6–9 with Figure 4A, lanes 6–10). Clearly, messengers ending at pA1 or pA2 do not differ in their behavior under these conditions.

pA site usage during growth factor induction

The mouse DHFR gene contains four possible pA sites. Upstream pA sites have been shown to be favored in growing cells (22). To study whether c-*myc* pA site usage might be modulated during GF induction we analyzed RNA from quiescent and GF-stimulated cells. Confluent Rat-2 and NRK cell cultures were incubated in medium containing 0.5% serum for 3 days and were subsequently stimulated with medium containing 20% FCS.

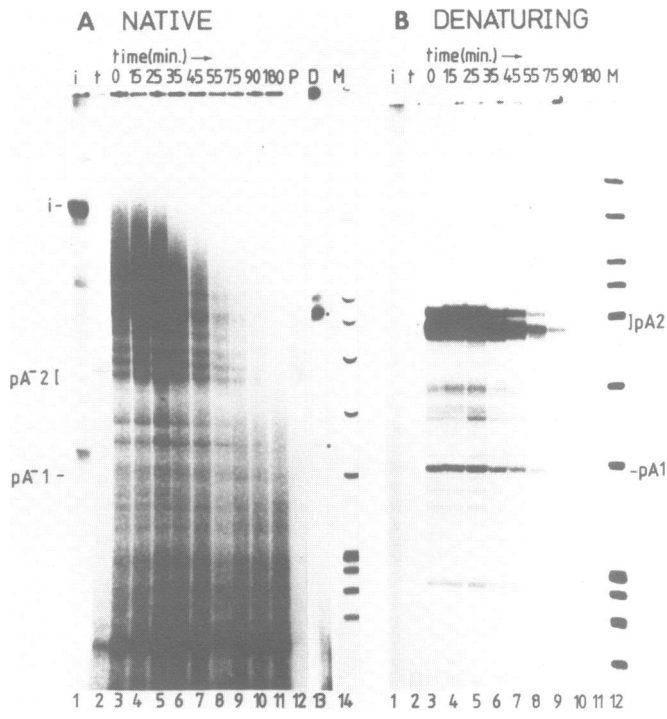

Figure 7. Analysis of poly(A) tail shortening. 40 μg cytoplasmic RNA from HeLa cells treated for various times with actinomycin D, was hybridized to the human 3′ c-*myc* probe. After RNase digestion and precipitation 80% of the sample was loaded onto a native gel (**A**) and 20% onto a denaturing gel (**B**). i: input probe; t: tRNA; P: nuclease P1 treated sample (5 μg HeLa RNA); D: sample denatured by boiling (5 μg HeLa RNA); M: marker: 517, 454, 396, 298, 220, 154, 145, 132, 118 nucletides (neglect first 2 bands in denaturing gel, as they are incomplete digestion products). Exposure: 14 hrs for both gels.

RNA was isolated at various timepoints after GF induction. The result was the same for both cell types. The analysis of stimulated NRK cells is shown in Figure 6. c-*myc* mRNA levels start to increase after 30 minutes and are maximally induced (6×) at 90 minutes post induction. The addition of GFs caused an equal increase of mRNAs terminating at either pA site and did not lead to a change in the pA2/pA1 ratio. Thus the use of the two pA sites does not seem to be altered during GF induction.

Poly(A) tail shortening of c-myc mRNA

A recently described factor that may be involved in the regulation of mRNA stability is the rate of poly(A) tail shortening. Using a cell-free system to study mRNA decay, Brewer and Ross (25) showed that the poly(A) tail of c-*myc* mRNA is shortened as the messenger decays. They also detected 3′ degradation products following the loss of the poly(A) tail. Poly(A) tail shortening was seen *in vivo* for the c-*fos* messenger as well, using GF stimulated cells (24). By performing RNase protection experiments with RNA from actinomycin D treated cells (like the one shown in Figure 4) and loading the samples on a non-denaturing gel, we have investigated whether the loss of the c-*myc* poly(A) tail is also found *in vivo* and whether the rate of shortening is equal for the two types of c-*myc* mRNAs. RNA

samples from cells incubated with actinomycin D for various times were used for an RNase protection analysis as described above. After digestion, the samples were split in half and loaded on denaturing and non-denaturing polyacrylamide gels. In the native gel the protected probe fragment remains hybridized to the mRNA. Since the probe spans the complete 3′ end of the mRNAs and RNase T1 does not cleave A residues, the poly(A) tail will be present in the hybrids. The result is shown in Figure 7. On the native gel, the bulk of c-*myc* mRNA, ending at pA2, gives rise to a long smear extending upwards of the expected position. Indeed, this smear becomes shorter as time passes. The predicted position of poly(A)$^-$ *myc* messengers can be concluded from the double-stranded DNA markers. Treatment of samples with nuclease P1 leads to removal of the poly(A) tail. The bands then migrate at the predicted position (not shown). This has been attempted with the sample in lane P but the digestion was not complete. Single-stranded RNA migrates much more slowly than double-stranded molecules of the same length, as can be seen in lane D, where the sample was heat-denatured prior to loading. The autoradiogram shown in Figure 7A was scanned densitometrically and the area under the peak due to the poly(A) tail smear was integrated. The obtained values were plotted logarithmically against the time (not shown). The calculated half-life of the pA2 smear is about 14 min. Thus it appears that the time it takes for the poly(A) tail to be degraded correlates well with the half-life of total c-*myc* mRNA. Due to a high background and low levels of transcripts ending at pA1, we cannot detect if, and how rapidly, these transcripts lose their poly(A) tail. However, we have shown that the half-life of pA1 and pA2 messengers is comparable and therefore we suspect that the poly(A) tails of both types of mRNA are degraded with the same kinetics.

DISCUSSION

No apparent cell type or differentiation stage specificity of pA site usage

The c-*myc* gene contains 2 pA signals, highly conserved between rat and man. (Dual pA sites have also been been described for the chicken c-*myc* gene (38). Its sequence, however, was not available to us.) We postulated that the presence of 2 pA signals might have a regulatory function. Others have shown that the second pA site, pA2, is used most often in human cells (24,36,37) and exclusively in rat (33) and chicken cells (38). We found a pA2/pA1 ratio of about 6 in all human and rat cells examined, whether they were from embryonal origin (HEL, HER, REF) or from more differentiated tissues, or contained a c-*myc* amplification (COLO 320, M13). Nishikura *et al.* estimated the pA2/pA1 ratio to be 20 in 3 Burkitt lymphoma cell lines. This conclusion was drawn from data obtained by scanning an autoradiogram. Our experience is that scintillation counting of bands excised from a gel provides a more accurate quantitation of bands differing strongly in intensity, such as the pA1 and pA2 bands. Hayashi *et al.* could not detect a pA1 band in rat cells. Whether this discrepancy with our results is due to the differences in cell lines or tissues, or to the differences in detection procedures, is unknown. In summary, pA2/pA1 ratios were comparable in all the cells we analyzed, even in rat cells containing the human gene. The only exception published to date is the expression of human c-*myc* in *Xenopus* oocytes (37), where both pA sites were used with equal efficiency. However, in these cells only a fraction of the RNAs was spliced correctly, indicating that post-transcriptional processes were not necessarily normal.

mRNAs ending at both pA sites do not behave differently

The c-*myc* mRNAs with different 3′ termini are equally unstable. Upon treatment of cells with CH or GFs, the levels of pA1 and pA2 mRNAs increase proportionally. Therefore,

under the conditions studied there does not seem to be a difference in behavior between pA1 and pA2 mRNA. We also tried to examine whether the poly(A) tail of the two RNAs was shortened. The shortening of the poly(A) tail of pA2 messengers was clearly visible and the time necessary for complete poly(A) tail loss correlated well with the determined half-life of c-*myc* mRNA. This suggests that loss of the poly(A) tail is the rate limiting step in mRNA decay. Our findings are in agreement with the mRNA degradation model proposed by Wilson and Treisman (24) who postulate that loss of the poly(A) tail precedes rapid degradation of the rest of the mRNA. An unusual feature of the pA2 smear, visible in Figure 7, was its strange banded pattern. This could be caused by the fact that poly(A) tail degradation takes place in spurts, or that RNAs carrying short tails migrate aberrantly due to an altered secondary structure.

What determines the preference for pA2?

Since mRNAs ending at both termini are equally unstable, the overabundance of pA2 messengers must be determined by preferential cleavage and polyadenylation. This could be caused by cell-specific factors that either favor certain sequences surrounding a pA site or preferentially use pA sites dependent on their location. It could also simply be a consequence of the mechanism of pA site recognition. Interesting experiments were performed by Denome and Cole (39), who studied polyadenylation using constructs containing several repeats of the same pA signal. Based on their findings they postulate that the polyadenylation factor scans the nascent RNA chain in the 3′ to 5′ direction and uses the first pA site it encounters. The ratio between the pA sites used would then be determined by the distance between consecutive pA sites. This is in accordance with our observation that the presence of the SV40 pA signal 250 bp downstream of c-*myc* pA2 causes a decrease in pA2 mRNA but does not seem to affect the amount of pA1 messengers (Figure 3B). Thus it is possible that one of the reasons why more c-*myc* mRNA terminates at pA2 is that the distance between the two pA sites is small (150 bp). However, as the sequences surrounding each pA signal are not alike one may assume that the affinity of the poly(A) addition machinery for each site also plays a role. We are in the process of constructing several c-*myc* pA deletion and exchange mutants which should provide more information on this subject.

Why 2 pA sites?

Why the c-*myc* gene should have 2 pA sites remains an unanswered question. Both types of mRNA encode the same proteins and we have been unable to find regulatory differences between usage of the sites or the mRNAs derived from them. Yet the fact remains that both signals have been conserved. Possibly the circumstances under which differential use of the c-*myc* pA signals has a regulatory function have not yet been found. Modulation of pA site usage of the chicken vimentin gene was only found during erythroid development. Another gene that contains more than one pA signal and several (A+T)-rich regions is the c-*jun* protooncogene. Transcription of the gene gives rise to two mRNAs of different lengths (40). The cell lines analyzed to date contain both c-*jun* transcripts. It has been shown that (A+T)-rich regions play a role in destabilizing mRNA. The AT1 region of c-*myc* is present in all mRNAs. Jones and Cole (13) have made deletions in the 3′ part of the c-*myc* gene showing that loss of a fragment containing AT1 stabilizes the resulting mRNAs. However, in their mutants the c-*myc* stop codon has been lost and they fail to show that the produced mRNAs terminate at pA2. It has not been proven that the AT1 region can confer instability on the longer transcripts. Perhaps the distance between the (A+T)-rich region and the poly(A) tail is of importance. That would explain the necessity

of a second (A+T)-rich region close to pA2. We hope to shed some light on this matter using AT2 deletion mutants.

ACKNOWLEDGEMENTS

The authors would like to thank S. Cory and G. Klein for the human and rat c-myc genes, P. Laird for the pEP plasmids, M. Timmers, M. Wurfbain and T. Berkvens for donating various RNAs, F. Cuzin for supplying the REF-Py cells, T. Jones and M. Cole for a technical tip on the RNase protection assay and T. Wand for photographing the figures. Furthermore we wish to thank Hans Bos, Sander van den Heuvel, Hans van Ormondt, Marc Timmers and Alt Zantema for critically reading the manuscript and giving useful suggestions.

REFERENCES

1. Alitalo,K., Koskinen,P., Makela,T.P., Saksela,K., Sistonen,L. and Winqvist,R. (1987) Bioch. Bioph. Acta, **907**, 1–32.
2. Yang,J.-Q., Remmers,E.F. and Marcu,K.B. (1986) EMBO J., **5**, 3553–3562.
3. Remmers,E.F., Yang,J.-Q. and Marcu,K.B. (1986) EMBO J., **5**, 899–904.
4. Bentley,D.L. and Groudine,M. (1986) Nature, **321**, 702–706.
5. Eick,D. and Bornkamm,G.W. (1986) Nucleic Acids Res., **14**, 8331–8346.
6. Caput,D., Beutler,B., Hartog,K., Thayer,R., Brown-Shimmer,S. and Cerami,A. (1986) Proc. Natl. Acad. Sci. USA, **83**, 1670–1674.
7. Shaw,G. and Kamen,R. (1986) Cell, **46**, 659–667.
8. Kelly,K., Cochran,B.H., Stiles,C.D. and Leder,P. (1983) Cell, **35**, 603–610.
9. Greenberg,M.E. and Ziff,E.B. (1984) Nature, **311**, 433–438.
10. Dani,C., Blanchard,J.M., Piechaczyk,M., El Sabouty,S., Marty,L. and Jeanteur,P. (1984) Proc. Natl. Acad. Sci. USA, **81**, 7046–7050.
11. Kruijer,W., Cooper,J.A., Hunter,T. and Verma,I.M. (1984) Nature, **312**, 711–716.
12. Müller,R., Bravo,R., Burckhardt,J. and Curran,T. (1984) Nature, **312**, 716–720.
13. Jones,T.R. and Cole,M.D. (1987) Mol. Cell. Biol., **7**, 4513–4521.
14. Rahmsdorf,H.J., Schönthal,A., Angel,P., Litfin,M., Rüther,U. and Herrlich,P. (1987) Nucleic Acids Res., **15**, 1643–1659.
15. Fort,P., Rech,J., Vie,A., Peichaczyk,M., Bonnieu,A., Jeanteur,P. and Blanchard,J.-M. (1987) Nucleic Acids Res., **15**, 5657–5667.
16. Kabnick,K.S. and Housman,D.E. (1988) Mol. Cell. Biol., **8**, 3244–3250.
17. Battey,J., Moulding,C., Taub,R., Murphy,W., Stewart,T., Potter,H., Lenoir,G. and Leder,P. (1983) Cell, **34**, 779–787.
18. Gazin,C., Dupont De Dinechin,S., Hampe,A., Masson,J.-M., Martin,P., Stehelin,D. and Galibert,F. (1984) EMBO J., **3**, 383–387.
19. Berget,S.M. (1984) Nature, **309**, 179–182.
20. Leff,S.E., Rosenfeld,M.G. and Evans,R.M. (1986) Ann. Rev. Biochem., **55**, 1091–1117.
21. Zehner,Z.E. and Patterson,B.M. (1983) Proc. Natl. Acad. Sci. USA, **80**, 911–915.
22. Kaufman,R.J. and Sharp,P.A. (1983) Mol. Cell. Biol., **3**, 1598–1608.
23. Linial,M., Gunderson,N. and Groudine,M. (1985) Science, **230**, 1126–1132.
24. Wilson,T. and Treisman,R. (1988) Nature, **336**, 396–399.
25. Brewer,G. and Ross,J. (1988) Mol. Cell. Biol., **8**, 1697–1708.
26. Klein,B., Pastink,A., Odijk,H., Westerveld,A. and Van Der Eb,A.J. (1989) submitted for publication.
27. Alitalo,K., Schwab,M., Lin,C.C., Varmus,H.E. and Bishop,J.M. (1983) Proc. Natl. Acad. Sci. USA, **80**, 1707–1711.
28. Topp,W.C. (1981) Virol., **113**, 408–411.
29. De Larco,J.E. and Todaro,G.J. (1978) J. Cell. Physiol., **94**, 335–342.
30. Adams,J.M., Gerondakis,S., Webb,E., Corcoran,L.M. and Cory,S. (1983) Proc. Natl. Acad. Sci. USA, **80**, 1982–1986.
31. Maniatis,T., Fritsch,E.F. and Sambrook,J. (1982) Molecular Cloning: A Laboratory Manual. Cold Spring Harbour Laboratory Press, Cold Spring Harbour.

32. Gorman,C.M., Moffat,L.F. and Howard,B.H. (1982) Mol. Cell. Biol., **2**, 1044–1051.
33. Hayashi,K., Makino,R., Kawamura,H., Arisawa,A. and Yoneda,K. (1987) Nucleic Acids Res., **15**, 6419–6436.
34. Fort,P., Marty,L., Piechaczyk,M., El Sabrouty,S., Dani,C., Jeanteur,P. and Blanchard,J.M. (1985) Nucleic Acids Res., **13**, 1431–1442.
35. Brands,J.H.G.M., Maassen,J.A., Van Hemert,F.J., Amons,R. and Möller,W. (1986) Eur. J. Biochem., **155**, 167–171.
36. Swarwout,S.G., Preisler,H., Guan,W. and Kinniburgh,A.J. (1987) Mol. Cell. Biol., **7**, 2052–2058.
37. Nishikura,K., Goldflam,S. and Vuocolo,G.A. (1985) Mol. Cell. Biol., **5**, 1434–1441.
38. Nottenburg,C. and Varmus,H.E. (1986) Mol. Cell. Biol., **6**, 2800–2806.
39. Denome,R.M. and Cole,C.N. (1988) Mol. Cell. Biol., **8**, 4829–4839.
40. Ryseck,R.-P., Hirai,S.I., Yaniv,M. and Bravo,R. (1988) Nature, **334**, 535–537.
41. Devereux,J., Haeberli,P. and Smithies,O. (1984) Nucleic Acids Res. **12**, 387–395.

This article, submitted on disc, has been automatically converted into this typeset format by the publisher.